Probing the Molecular Primary and Secondary Structures of Saturated Hydrocarbons by X-ray Photoionization Spectroscopy

M. Deleuze,† J. Delhalle,*,† B. T. Pickup,‡ and S. Svensson§

Contribution from the Laboratoire de Chimie Théorique Appliquée, Facultés Universitaires Notre-Dame de la Paix, B-5000 Namur, Belgium, Department of Chemistry and Center for Molecular Materials, The University, Sheffield S3 7HF, United Kingdom, and Department of Physics, Uppsala University, Box 530, S-751 21 Uppsala, Sweden

Received January 25, 1994®

Abstract: The dependence of X-ray photoionization spectra on molecular structure characteristics is assessed by comparing Al Kα photoelectron results obtained in the gas phase for *n*-pentane, *n*-hexane, cyclopentane, and cyclohexane to many-body Green's function theoretical simulations coping with the leading correlation and relaxation effects. Both the experimental spectra and their simulations exhibit obvious signatures for changes in the molecular configuration and conformation. The comparison of theory with experiment corroborates nicely disordering effects in gaseous samples of the *n*-alkane compounds. Cyclohexane, on the contrary, is found to exist essentially in its chair conformation. It gives evidence for a weak but significant breakdown of the molecular picture above an approximate threshold of 24 eV in the inner valence region of medium-size saturated hydrocarbons, in particular cycloalkanes. Vibronic coupling effects are also found to affect strongly the outermost ionization photoelectron band of cyclopentane. As a direct application, inner- and outer-valence XPS results are used to probe the secondary structure of macromolecular chains at the extreme surface of lamellar microcrystals of polyethylene. The identified leading fold-stacking sequences are found to match the patterns of Reneker and Geil.

Introduction

Photoelectron spectroscopy studies are routinely used to obtain information on the chemical composition, bonding, and homogeneity of polymer surfaces, but rarely to extract information on their molecular structure, although the latter determines important properties like interfacial mixing, surface tension, adhesion, chemistry−biological response relationships of materials, etc. Based on theoretical predictions,[1] a recent experimental study[2] on polyetheylene crystalline and amorphous films has given evidence that changes in the secondary structure of the polymer chains at the sample surface can be traced in the valence region of the XPS spectra. Owing to the experimental conditions used (monochromatized Al $K\alpha_{1,2}$ X-rays at normal incidence on a HP5950 spectrometer), these results are still preliminary. Nevertheless they have played a crucial role in the interpretation[3] of the so far unexplained difference in the relative XPS intensities of the two C_{2s} peaks in *n*-tridecane ($C_{13}H_{28}$) when recorded in the gas and solid phases.

Previous works[4] have shown the value of studying gas phase model molecules to provide a detailed analysis of the core level structure of polymers. Their virtue resides not only in the higher resolution achieved in the gas phase but also in the separation of intramolecular characteristics (chemical bonding, vibrational influences on the line profiles, origin of the nonstoichiometric ratios of peak areas) from intermolecular interactions (polarization of neighboring molecules, phonon broadening, structural disorder, etc.) and solid state related effects limiting the resolution (surface charging). In this contribution, we carry out a similar investigation for alkane chains and polyethylene by analyzing the valence levels of gas phase *n*-pentane, cyclopentane, *n*-hexane, and cyclohexane. The main purpose is to use high-resolution valence XPS measurements to study the changes induced in the electronic structure by different molecular connectivities.[5]

This study also contributes to casting the type of information on the molecular conformation that could be accessible from the analysis of valence XPS spectra. To determine whether this approach can add to the relatively few effective methods (STM, AFM, NEXAFS, etc.) capable of directly probing the surface molecular structure of thin and ultrathin polymer films, theoretical calculations are used to interpret the experimental results and identify the electronic factors responsible for the sensitivity to geometry. As a byproduct of this investigation, we will therefore also refine some conclusions drawn previously[1b] from valence XPS spectra of crystal grown polyethylene with controlled morphologies.[6]

The molecules we are investigating in this work have been selected for their relevance to the recent results on crystalline and amorphous polyethylene films.[1,2] As schematically pictured in Figure 1, polyethylene crystals are composed of long chains, typically 500 nm, which organize in lamellae of which the thickness ranges typically from 10 to 20 nm.[6] At the molecular level, a polyethylene lamella consists of a bulk domain, in which

† Facultés Universitaires Notre-Dame de la Paix.
‡ The University.
§ Uppsala University.
® Abstract published in *Advance ACS Abstracts,* October 15, 1994.

(1) (a) Delhalle, J.; Delhalle, S.; Riga, J. *J. Chem. Soc., Faraday Trans. 2* **1988**, *83*, 503. (b) Deleuze, M.; Denis, J. P.; Delhalle, J.; Pickup, B. T. *J. Phys. Chem.* **1993**, *97*, 5115. (c) Deleuze, M.; Delhalle, J.; Pickup, B. T. *Chem. Phys.* **1993**, *175*, 427.

(2) Delhalle, J.; Riga, J.; Denis, J. P.; Deleuze, M.; Dosière, M. *Chem. Phys. Lett.* **1993**, *210*, 21.

(3) Riga, J.; Delhalle, J.; Deleuze, M.; Pireaux, J. J.; Verbist, J. J. *Surf. Interface Sci. Anal.* In press.

(4) (a) Brito, A. N. d.; Keane, M. P.; Correia, N.; Svensson, S.; Gelius, U. *Surf. Interface Sci. Anal.* **1991**, *17*, 94. (b) Brito, A. N.d.; Correia, N.; Svensson, S.; Agren, H. *J. Chem. Phys.* **1991**, *95*, 2965. (c) Beamson, G.; Briggs, D. *Mol. Phys.* **1992**, *76*, 919. (d) Brito, A. N. d.; Svensson, S.; Agren, H.; Delhalle, J. *J. Electron Spectrosc. Rel. Phenom.* **1993**, *63*, 239−251.

(5) Deleuze, M.; Delhalle, J.; Pickup, B. T. *J. Phys. Chem.* **1994**, *98*, 2382.

(6) Dosière, M. Crystal Growth in Polyethylene. In *Handbook of Polymer Science and Technology*; Chereminisoff, N. P., Ed.; Marcel Dekker: New York, 1979, and references therein.

0002-7863/94/1516-10715$04.50/0

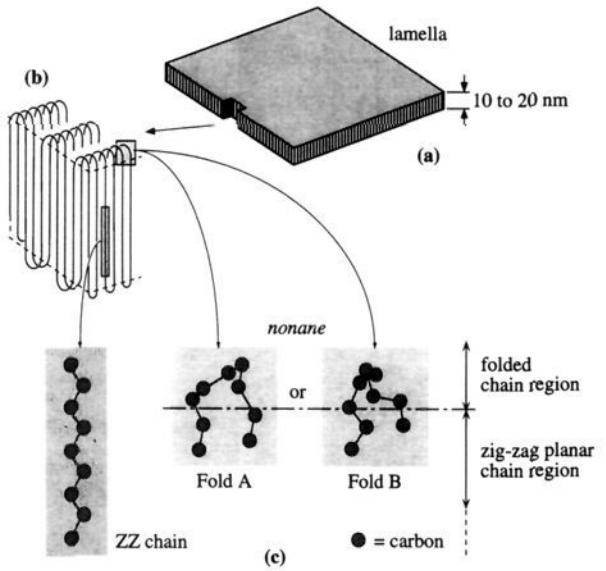

Figure 1. (a) Schematic drawing of lamellar crystals of polyethylene, (b) details showing the *all-trans* (zigzag planar) section and the fold region of the lamella, and (c) three conformations of *n*-nonane mimicking the folded and zigzag planar regions of the lamella.

chains in a zigzag planar conformation are oriented parallel, confined between two regions where the chains twist back to the bulk. The most important consequence is that the lamellae surfaces are rich in folded structures and, owing to the particular escape depth of X-ray photoelectrons (1−10 nm), constitute interesting samples for testing the sensitivity of the valence region to conformational changes.

One limitation with lamellae is that the folds might adopt different conformations,[7] the proportion of which is hard to define, even if there is evidence for order[8] imposed by the relative arrangement of the zigzag planar chains in the bulk.[9] This is why, in the present study, we have chosen to consider normal and cyclic pentane and hexane, which are of very close chemical nature and nearly isomeric pairwise, but strongly differ in their connectivity. They are also related to the fold question on polyethylene crystals in as much as they can be considered as conformational prototypes of the chains in the bulk and at the surface of lamellae, respectively, for the *all-trans* and the cyclic pentane and hexane.

Theory: Model Systems and Computational Aspects

Photoelectron spectra of *n*-pentane, cyclopentane, *n*-hexane, and cyclohexane have been computed on the basis of RHF/STO-3G optimized geometries which, in a systematic study conducted on cycloalkanes,[5] were found to be consistent with experiment and several force field or higher level *ab initio* calculations. The *all-trans* conformation, which is prevailing for *n*-alkanes, has been selected for *n*-pentane (**TT**) and *n*-hexane (**TTT**). To evaluate the outcome of molecular disorder in the gas phase, the trans-gauche-trans form (**TGT**) of *n*-hexane has also been taken into consideration. Although the envelope (**E**) and half-chair (**HC**) conformations of cyclopentane differ by less than 3 kJ·mol^{-1} and henceforth compose a very mobile mixture in the gas phase, only the former structure has been considered: for these two conformers interconverting nearly freely through the planar form as a saddle point, the successive twists along the pseudorotation path do not disturb significantly their electronic structure.[5] The molecular structure of cyclohexane is usually discussed in terms of three conformations: the classical and rigid chair (**C**) form, and the flexible twisted-boat (**TB**) and boat (**B**) forms, the latter two being less stable than **C** by 24 and 28 kJ·mol^{-1}. It is therefore natural to simulate gaseous samples of cyclohexane at room temperature in terms of the **C** form only. To detect some XPS features fingerprinting a hypothetical ring inversion, we will also consider the **TB** conformation of cyclohexane. The molecular structures studied are shown in Figure 2, and the details on their geometrical parameters can be found in ref 5.

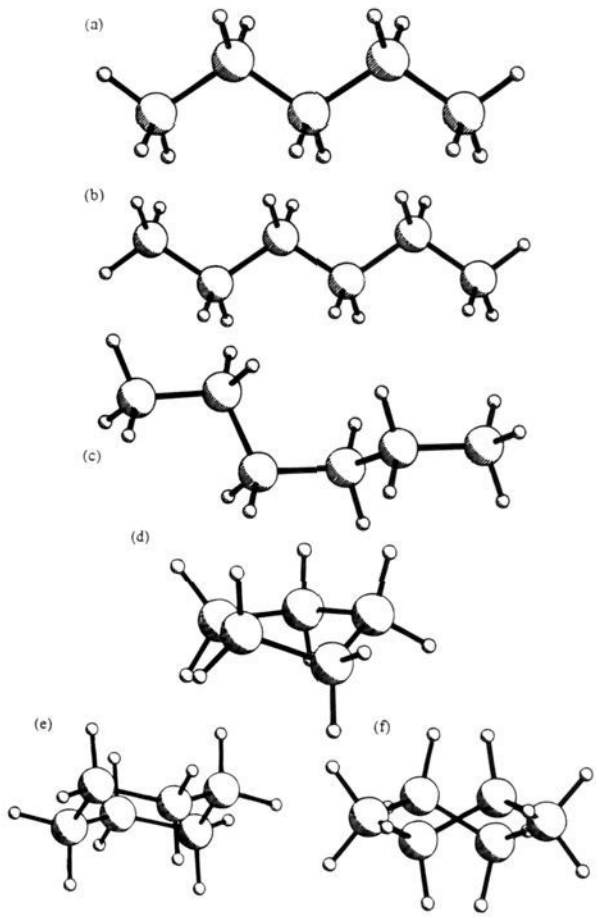

Figure 2. Selected structures: (a) *n*-pentane in the trans-trans (**TT**) conformation; *n*-hexane in (b) the trans-trans-trans (**TTT**) and (c) trans-gauche-trans (**TGT**) conformations; (d) cyclopentane in the envelope (**E**) conformation; cyclohexane in (e) the chair (**C**), (f) the twisted-boat (**TB**), and the boat (**B**) conformations.

Experimental spectra will be interpreted on the basis of Koopmans' and Many-Body Green's Function[10] results, obtained using several decoupling schemes. Comparisons already carried out on linear alkanes[1c] indicate that the renormalized expression of the second-order self-energy in the so-called diagonal 2ph-TDA/QP (two-particle-hole Tamm-Dankoff Approximation/

(7) (a) Keller, A. *Phil. Mag.* **1957**, *2*, 1171. (b) Flory, P. J. *J. Am. Chem. Soc.* **1962**, *84*, 1857. (c) Fischer, E. W., Goddas, H.; Schmidt, G. F. *Polym. Lett.* **1967**, *5*, 619. (d) Georgeadis, G.; St. John Marley, R. *Polym. Lett.* **1971**, *9*, 297. (e) Fischer E. W., Lorentz, R. *Kolloïd Z. Z. Polym.* **1963**, *189*, 97.

(8) Blackadder, D. A.; Roberts, T. L. *Die Makromol. Chem.* **1969**, *126*, 116.

(9) (a) Keller, A. *Phil. Mag.* **1957**, *2*, 1171. (b) Wunderlich, V. *Macromolecular Physics*; Academic Press: London, 1973; Vol. 1. (c) Avitabile, G.; Napolitano, R.; Pirozzi, B., Rouse, K. D.; Thomas, M. W.; Willis, B. T. M. *Polym. Lett.* **1975**, *13*, 351. (d) Tadokoro, H. *Structure of Crystalline Polymers*; Wiley: New York, 1979.

(10) (a) Öhrn, Y.; Born, G. *Adv. Quantum Chem.* **1981**, *13*, 1 and references therein. (b) M. Deleuze, Etude de la Structure Electronique de Chaînes Modèles par l'Approche en Propagateurs à une Particule, Ph.D. Thesis (Namur, FUNDP, 1993), and references therein.

quasi-particle) scheme leads to a reliable reproduction of the main XPS spectral characteristics (position, width, and shape of bands) in the inner-valence energy region. This approach has been preferred to other schemes of decoupling such as the second-order (MBGF2) or Shifted Born Collision (SBC) approximations for the self-energy, since for linear alkanes, it has allowed the calculation of the relative positions of inner-valence ionization lines within less than 4% of error with respect to experiment. Even in the limit of an infinite stereoregular polymer, the ionization spectra of saturated hydrocarbons can be consistently interpreted[11] on the basis of a one-particle picture over nearly all the valence region. For such compounds for which the fundamental gap exceeds 12 eV,[12] shake-up lines and shake-off bands are of low intensity[13] and have to fall in a higher binding energy region than main lines (i.e. above an approximate threshold of 24 eV), which justifies in a first approximation the neglect of configuration mixing effects in the ionized system. Owing to the identical chemical nature of the systems considered in this work and those previously investigated[1,5] and the similarity of the questions addressed, we feel rather confident in using the same level of description to analyze the gas phase data on *n*-pentane, cyclopentane, *n*-hexane, and cyclohexane. It is useful to recall that configurational and conformational signatures in the XPS spectra of saturated hydrocarbons essentially find their origin in the nodal characteristics of the molecular orbitals. These signatures can therefore be consistently analyzed[1b] in terms of the relative distribution of main lines, which appears to be mostly unaffected by basis set effects (see ref 1c and references therein).

The Hartree–Fock (HF) calculations have been carried out using the Gaussian 82 series of programs[14] with the STO-3G basis—the requested convergence on the density matrix being fixed to 10^{-8} and the integral cutoff to 10^{-10} hartree. Many-body corrections to the Koopmans results have been calculated with a homemade program. Photoionization intensities have been evaluated using the parametric Gelius model[15] for molecular orbital cross sections; the relative atomic photoionization cross sections used for C_{2s}, C_{2p}, and H_{1s} being 100.0, 7.69, and 0.00, respectively (core atomic functions do not significantly participate in the molecular orbitals of the valence region). Although this simple model implies the use of a minimal basis set, it reflects nicely[1c] the influence of the C_{2s}–C_{2p} mixing of states at the border of the inner- and outer-valence regions arising with the development of methylenic hyperconjugation effects[1b] on the calculated photoionization intensities. For a better account of many-body effects, the Gelius cross sections, obtained from an uncorrelated model, are multiplied by the corresponding pole strength factors Γ_c as obtained from a Green's function calculation. More details on the technical aspects of these calculations can be found in ref 1c.

Simulated XPS spectra are constructed from a superposition of peaks centered at the Koopmans and 2ph-TDA/QP values for electron binding energies, respectively. The line widths of the electron bands in the inner-valence region of the molecules in this study are not determined by the resolution of the spectrometer, which by a measurement on Ar 3p calibration lines was found to be 0.45 eV. Instead, vibrational broadening is one of the most important factors behind the line widths. However, the molecules are very large and therefore the vibrational line shape is very difficult to simulate theoretically. In order to give a guide-to-the-eye line that can be compared with the experimental spectra, we have chosen to convolute our theoretical spectra using a spread function with a full width at half maximum of 1.1 eV, the peak heights being scaled according to the intensity previously computed. The value 1.1 eV was taken as an average width when looking at the experimental results.

Experimental Section

The XPS spectra for the model molecules were recorded on a high-resolution X-ray photoelectron spectrometer for gas phase measurements using monochromatized Al $K\alpha_{1,2}$ X-rays ($h\nu$ = 1486.6 eV) to excite the spectra.[16] This instrument comprises a quartz crystal monochromator, multidetection of the electrons, and a two-stage differentially pumped gas cell. The pressure in the gas cell was maintained below 2.0 mbar in order to avoid any possible effects of inelastic scattering contribution to the spectra. The pass energy of the analyzer was kept at 200 eV, and the instrument resolution at this energy was measured on calibration with Ar 2p and Ar 3p photoelectron lines to be 0.45 eV. The photoionization cross section, using 1486.6 eV photon energy, in the valence photoelectron region for these compounds is very weak and therefore typical recording times were several hours. Several runs were made on each spectrum. Calibration was made by using the Ar $2p_{3/2}$ line at 248.63 eV[17] and Ar 3p line at 15.80 eV.[18] Ar gas was mixed with the sample gas and the core lines were recorded simultaneously in the calibration procedure. A check of the calibration energies was also made by a comparison of prominent structures in the outer C_{2p} valence region with the values given by Kimura et al.[19]

The four compounds studied are high-purity *n*-pentane (Aldrich 15495-4: 99%), cyclopentane (Merck 2598: 99.8%), *n*-hexane (Merck 2500: 99%), and cyclohexane (Merck 2822: 99.8%). A search for possible contaminants was made by checking the O_{1s}, N_{1s}, and C_{1s} regions. No contaminant core photoelectron lines were found.

The SCIENTA[20] data analysis program was used to fit Gaussian lines to the structures in the spectra. The profile of the main inner valence photoelectron lines is mainly due to vibrational excited singly ionized final states. The systems studied in this report contain more than 15 atoms resulting in a large number of normal vibrations, making a complete vibrational analysis of the photoelectron line profiles difficult and certainly outside the experimental resolution, even in the case of monochromatized XPS at 1486.6 eV photon energy. In this report we discuss the differences in the band profiles when comparing the different molecules. Therefore we restricted the number of parameters in the curve fitting by using only symmetric Gaussians where the free parameters were the line widths, the line positions, and the peak intensities.

Results and Discussion

The simulated spectra of the selected compounds are displayed in Figure 3 at the Koopmans and diagonal 2ph-TDA/QP levels of approximation. In the latter case, the photoionization main lines are also given as a spike spectrum. Strong dynamic relaxation effects yield a shift and contraction of bands toward lower binding energies. Except for this and for the concomitant dispersion of photoionization intensity to satellite structures, the Koopmans and diagonal 2ph-TDA/QP spectra

(11) Liegener, C. M. *Chem. Phys. Lett.* **1990**, *167*, 555.
(12) Mort, J.; Pfister, G. *Electronic Properties of Polymers*; Wiley: New York, 1982.
(13) Cederbaum, L. S.; Domcke, W.; Schirmer, J.; Von Niessen, W.; Diercksen, G. H. F.; Kraemer, W. P. *J. Chem. Phys.* **1978**, *69*, 1592.
(14) Frisch, M. J.; Binkley, J. S.; Schlegel, H. B.; Raghavachari, K.; Martin, R. L.; Martin, R. A.; Stewart, J. J. P.; Bobrowicz, F. W.; DeFrees, D. J.; Seeger, R.; Whiteside, R. A.; Fox, D. J.; Fleuder, E. M.; Pople, J. A. Gaussain 82, release C; Carnegie Mellon University: Pittsburgh, PA, 1984.
(15) Gelius, U *J. Electron Spectrosc. Rel. Phenom.* **1974**, 5, 985.
(16) Gelius, U.; Asplund, L.; Basilier, E.; Hedman, S.; Helenelund, K.; Siegbahn, K. *Nucl. Instrum. Methods* **1985**, *B1*, 85.
(17) King, G. C.; Tronc, M.; Read, F. H.; Bradford, R. C. *J. Phys.* **1977**, *B10*, 2479.
(18) Moore, C. E. *Atomic Energy Levels*; Natl. Bur. Stand. (U.S.) Circ. No. 467; U.S. GPO: Washington DC, 1949; Vol I.
(19) Kimura, K.; Katsumata, S.; Achiba, Y.; Yamazaki, T.; Iwata, S. *Handbook of Photoelectron Spectra of Fundamental Organic Molecules*; Japan Scientific Societies Press: Tokyo 1981.
(20) Program available in Scienta Instrum. AD, Uppsala, Sweden.

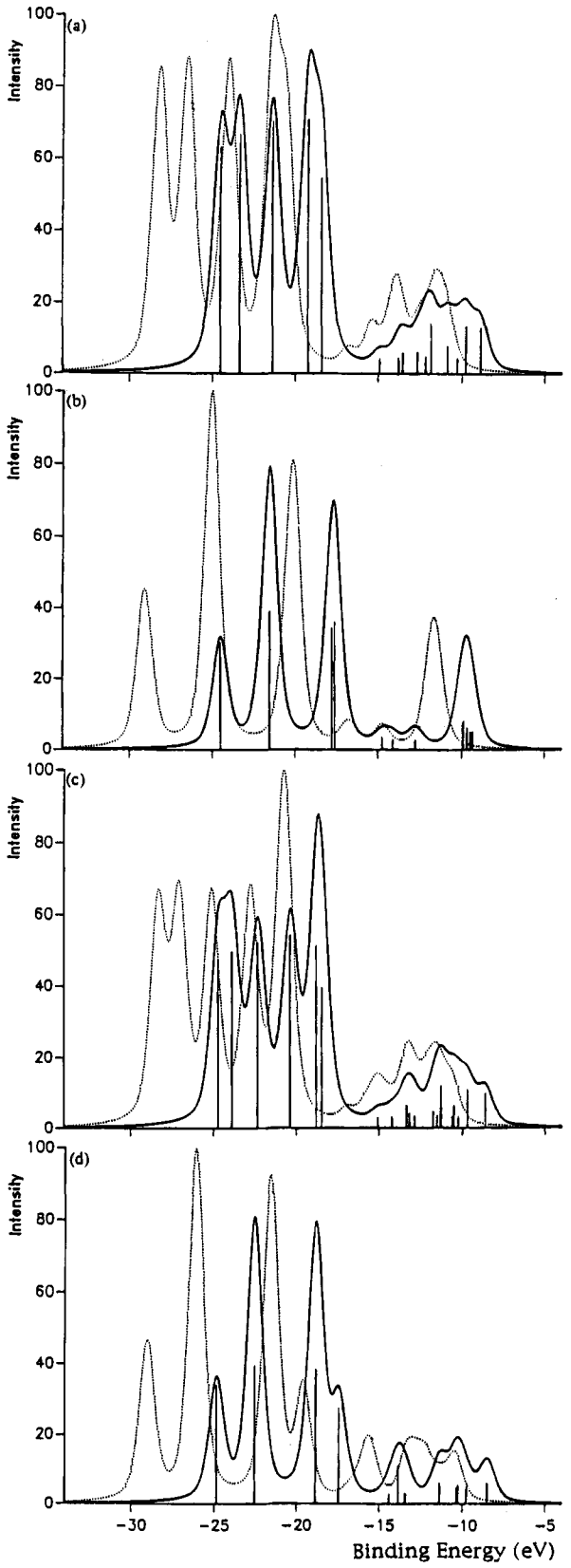

Figure 3. 3. Theoretical XPS spectra of (a) *n*-pentane in the **TT** form, (b) cyclopentane in the **E** form, (c) *n*-hexane in the **TTT** form, and (d) cyclohexane in the **C** form simulated at the Koopmans (···) and diagonal 2ph-TDA/QP (—) levels of approximation.

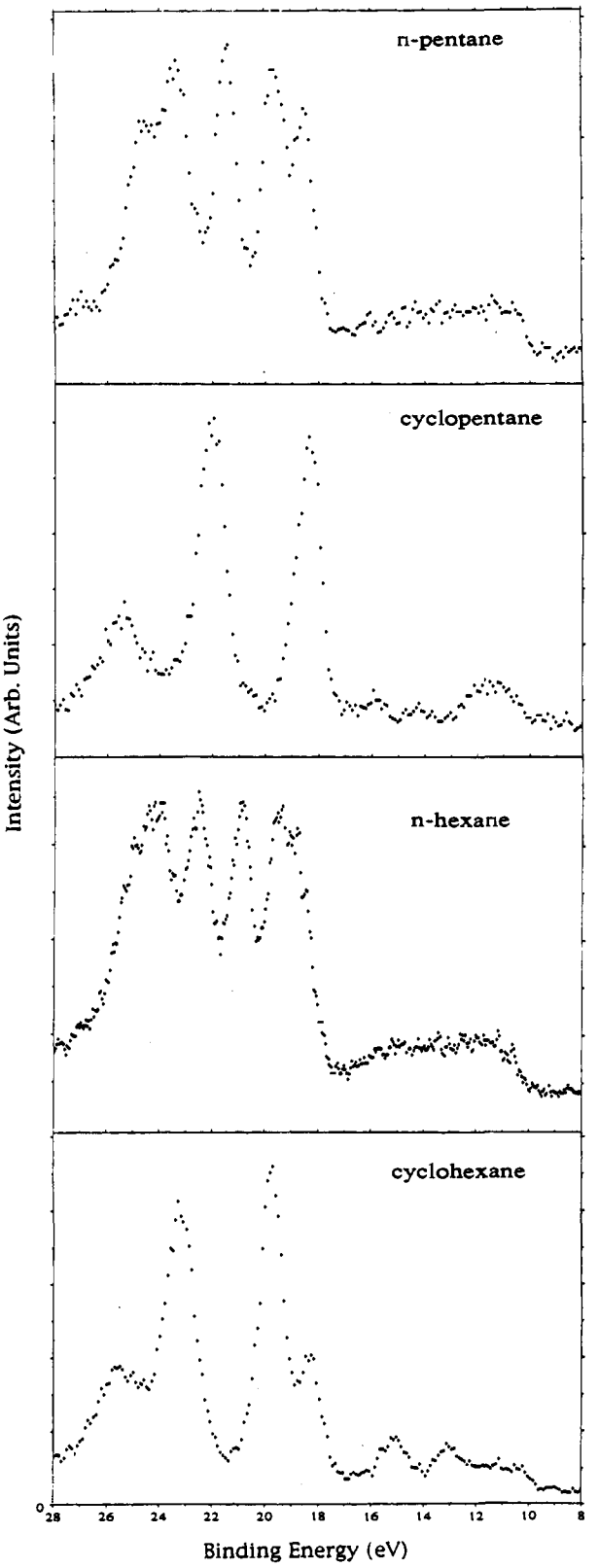

Figure 4. Experimental XPS spectra of (a) *n*-pentane, (b) cyclopentane, (c) *n*-hexane, and (d) cyclohexane.

are essentially similar, a result of the balance of counteracting many-body effects of quite different nature on the convoluted intensities.[21]

Our simulations nicely reproduce the general features in the experimental records obtained from the gas phase (Figures 4 and 5). In both the experimental and theoretical spectra, two bands of rather different intensity can be distinguished on the energy scale. This justifies the somewhat arbitrary[1b] classification of the valence molecular orbitals of a C_nH_{2n+2} [C_nH_{2n}] molecule into n inner-valence levels dominated by C_{2s} atomic

(21) (a) Deleuze, M.; Delhalle, J.; Pickup, B. T. *J. Electron. Spectrosc. Rel. Phenom.* **1992**, *60*, 37. (b) Delhalle, J.; Deleuze, M. *J. Mol. Struct. (Theochem)* **1992**, *261*, 187.

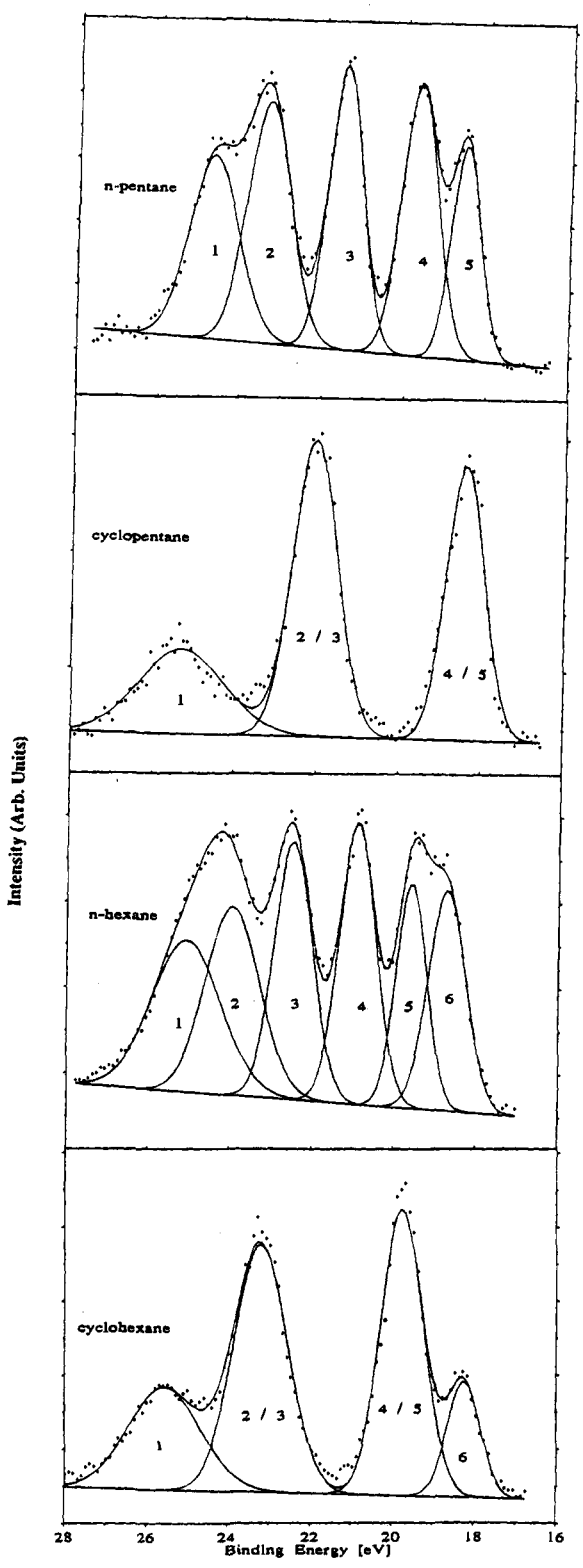

Figure 5. Deconvoluted XPS spectra (inner-valence region) of (a) *n*-pentane, (b) cyclopentane, (c) *n*-hexane, and (d) cyclohexane.

contributions and $2n + 1$ ($2n$) outer-valence levels of leading ($C_{2p} + H_{1s}$) character. The inner-valence STO-3G electron binding energies, calculated using several levels of approximation, can be compared to experimental data in Table 1. From the linear correlations displayed in Figure 6, one can readily evaluate the quality of the diagonal 2ph-TDA/QP results if only relative line positions are to be considered.

However, interesting discrepancies between the simulated spectra and the experimental records can be observed in the width and shape of some particular peaks. A safe interpretation of these disagreements would imply a complete analysis of secondary phenomena such as vibronic couplings or electronic configurational mixing effects in the final state, which is beyond the scope of this article. At this point, we restrict ourselves to qualitative considerations only.

A minimal STO-3G basis set yields shake-up states of artificially too high energy and tends therefore to limit the dispersion of photoionization intensity from primary lines to satellite secondary structures. For oligomers closely related to polyacetylene, the shake-up lines and shake-off bands recently have been found[22] to result in a strong correlation band, which grows up and merges progressively into the primary inner-valence band when the size of the system increases. Similarly, with saturated hydrocarbons and almost in the cases of cycloalkanes, the presence of a correlation tail might also be at the origin of a net broadening of the peaks appearing above 23–24 eV (Table 2), i.e. at the bottom of the inner-valence band. This could also explain the apparent borrowing of intensity in this energy region at the expense of the rest of the valence spectrum, in comparison (Table 2) to the uncorrelated theoretical values obtained for relative primary photoionization intensities. These observations are consistent with the STO-3G pole strength values obtained (Table 2), which indicate a stronger breakdown of the molecular picture for the ionization of the innermost levels of cyclopentane and cyclohexane compared to *n*-pentane and *n*-hexane, a trend that can be related to the larger dispersion of energy levels arising with the ring closure. Since for the compounds addressed the measured double ionization threshold lies around 30 eV, the correlation tail must be of pure shake-up nature.

Another interesting feature is the very strong broadening of the peak at the top of the outer valence band of cyclopentane in comparison to its simulated spectrum. For an ideal structure of D_{5h} symmetry, the six outermost ionization lines fall in three degenerate pairs within an energy interval centered at 9.70 eV and shorter than 0.3 eV. These energy degeneracies are only removed by a few hundredths of an electronvolt when cyclopentane resides in its **E** or **HC** conformation. This compound is thus a good candidate for a Jahn–Teller distorsion after the removal of one electron from its highest occupied level. As the ring is highly flexible, strong vibronic couplings may then yield fast rotating vibrations in the radical cation, which explains the broadening mentioned above and corroborates the conclusions drawn[23] from available electron spin resonance (ESR) spectra.

In spite of their limitation, either the calculated or the recorded spectra exhibit obvious differences from one compound to another, confirming the valence X-ray photoionization spectroscopy as a direct gauge of the bonding characteristics. Since the cyclization of a linear chain implies intimately related effects on the molecular configuration and conformation as a result of combined variations on the atomic connectivity and torsional constraints, this observation calls for a more systematic analysis.

XPS Fingerprints of the Molecular Configuration. In regard to their higher connectivity, resulting in stronger symmetry restrictions on the mixing of one-particle states, the X-ray photoionization spectra of cycloalkane compounds exhibit much-better-resolved structures than their open-chain counterparts in the inner valence region but remarkably also in the outer-valence region. The influence of the cyclic connectivity on the inner

(22) Keane, M. P.; Naves de Brito, A.; Correia, N.; Svensson, S.; Karlsson, L.; Wannberg, B.; Gelius, U.; Lunell, S.; Salaneck, W. R.; Lödlung, M.; Swanson, D. B.; MacDiarmid, A. G. *Phys. Rev. B* **1992**, *45*, 6390.

(23) Lunell, S.; Eriksson, L. A.; Fängström, T.; Maruani, J.; Sjöqvist, L.; Lund, A. *Chem. Phys.* **1993**, *171*, 119.

Table 1. Experimental and Theoretical Electron Binding Energies (in eV) of the Selected Alkane Compounds in the Inner-Valence Region[a]

molecule	peak (MO line)	exptl results gas phase XPS	theoretical results (STO-3G) Koopmans	MBGF2	SBC	diagonal 2ph-TDA
n-pentane	(1)	24.67	28.19	25.93	25.13	24.51
(TT conformer)	(2)	23.33	26.52	24.58	23.88	23.36
	(3)	21.48	24.02	22.37	21.80	21.37
	(4)	19.65	21.43	20.03	19.59	19.24
	(5)	18.51	20.56	19.22	18.77	18.42
cyclopentane	(1)	25.31	29.07	26.47	25.41	24.50
(E conformer)	2−3	22.07	26.00	22.98	22.17	21.52
	4−5	18.40	20.14	18.70	18.13	17.69
n-hexane	(1)	25.09	28.33	26.00	25.25	24.71
(TTT conformer)	(2)	23.95	27.07	25.00	24.33	23.85
	(3)	22.48	25.11	23.28	22.70	22.30
	(4)	20.92	22.75	21.17	20.69	20.35
	(5)	19.59	20.85	19.47	19.08	18.79
	(6)	18.72	20.56	19.17	18.75	18.44
n-hexane	(1)	25.09	28.34	25.97	25.25	24.71
(TGT conformer)	(2)	23.95	27.02	24.92	24.30	23.83
	(3)	22.48	25.12	23.26	22.71	22.30
	(4)	20.92	22.71	21.11	20.65	20.31
	(5)	19.59	21.31	19.90	19.48	19.18
	(6)	18.72	20.18	18.82	18.42	18.12
cyclohexane	(1)	25.55	29.03	26.46	25.54	24.84
(C conformer)	2−3	23.20	26.08	23.875	23.105	22.53
	4−5	19.74	21.54	19.86	19.275	18.85
	(6)	18.24	19.60	18.23	17.76	17.42
cyclohexane	(1)		28.98	26.36	25.47	24.75
(TB conformer)	2−3		26.00	23.78	23.04	22.46
	4−5		21.87−21.60	20.16−19.91	19.58−19.38	19.17−18.92
	(6)		18.84	17.54	17.11	16.79

[a] *x*−*y*−*z*: computer fitted values for peaks maxima. (*x*): effective quasiparticle binding energies.

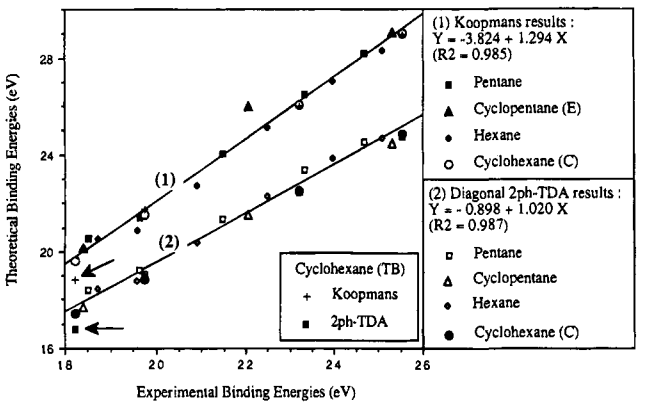

Figure 6. Correlation between the theoretical and experimental inner-valence binding energies. **TB** cyclohexane does not fit the average linear regression as well a **C** cyclohexane.

valence electronic structure can be simply rationalized in terms of a tight-binding or Hückel-like description, implying the assumption of the $C_{2s}-C_{2p}$ separability and the restriction of the $C_{2s}-C_{2s}$ combinations under an effective Hamiltonian to direct bonded neighbors. In the framework of these drastic approximations, the inner valence band of the selected compounds can be assimilated to the topological Hückel spectra[24] associated (Figure 7) with a chain or a cycle of 5 or 6 equivalent vertices.

Such a topological picture clearly illustrates the electronic degeneracies imposed in the inner valence region by the D_{5h} symmetry of planar cyclopentane or by the D_{3d} symmetry of cyclohexane in the **C** form. Indeed, both the experimental and theoretical spectra of cyclopentane exhibit three distinct structures in the inner-valence region. These can be directly related to the nondegenerate $1a_{1'}$ and doubly degenerate $1e_{1'}$ and $1e_{2'}$ sets of molecular orbitals for an ideal D_{5h} planar conformation. Similarly, one can find four resolved structures in the inner-valence band of cyclohexane corresponding in decreasing binding energy order to the $1a_{1g}$, $1e_g$, $1e_u$, and $1a_{2u}$ sets of molecular orbitals within a D_{3d} symmetry point group. In the outer-valence region of cyclopentane, three well-separated structures can also be distinguished either in the theoretical or in the experimental spectra. At least the simulation displayed for the **C** form of cyclohexane corroborates nicely the signals recorded for this compound in the outer-valence region, of which three distinct peaks clearly emerge in spite of the lower Al Kα photoionization cross section of the $(C_{2p} + H_{1s})$ molecular orbitals.

On the other hand, the lower C_{2v} or C_{2h} symmetry point groups of the all-staggered chains of *n*-pentane or *n*-hexane forbid any electronic degeneracy. It seems therefore natural to observe 5 or 6 resolved lines in the inner-valence spectra (Figure 5, a and c) recorded for *n*-pentane or *n*-hexane, respectively. Although the outer valence electrons of these compounds are distributed over 11 or 13 energy levels, they result in a poorly structured band of low intensity. In spite of this, our simulations are in line with data obtained in the solid phase[25] for the outer valence band of *n*-alkane compounds, which exhibits essentially two substructures.

XPS Fingerprints of the Molecular Conformation. In a tight-binding description from which the contribution of the directional atomic C_{2p} orbitals has been arbitrarily switched off, the torsional energetics more intimately related to conformational features is not considered. In the case of saturated hydrocarbons, this aspect of the molecular structure affects the electronic structure through the interplay of long-range methylenic hyperconjugation effects,[1b,1c,5] also referred to as σ-con-

(24) Trinastic, N. *Chemical Graph Theory*; C.R.C. Press, Inc.: Boca Raton, FL, 1993; Vol. I, Chapter 6.

(25) (a) Pireaux, J. J.; Caudano, R. *Am. J. Phys.* **1984**, *52*, 821. (b) Pireaux, J. J.; Svensson, S.; Basilier, E.; Malmqvist, P.-A.; Gelius, U.; Caudano, R.; Siegbahn, K. *Phys. Rev. A* **1976**, *14*, 2133.

Table 2. Theoretical vs Experimental Inner-Valence Photoionization Intensities and Related Parameters for the Selected Alkane Compounds

		theoretical results (STO-3G)		experimental results		
molecule	peak (MO line)	intensity (%)[a]	Γ_c[b]	height	fwhm (eV)	intensity (%)
n-pentane	(1)	20.7	0.7856	1430	1.418	20.3
(TT conformer)	(2)	21.1	0.8136	1880	1.220	22.9
	(3)	21.3	0.8470	2206	0.967	21.3
	(4)	20.9	0.8742	2117	1.029	21.8
	(5)	16.1	0.8730	1670	0.824	13.8
cyclopentane	(1)	19.6	0.6832	731	2.457	23.6
(E conformer)	2−3	43.9	0.7860	2560	1.259	42.4
	4−5	36.4	0.8497−0.8528	2372	1.089	34.0
n-hexane	(1)	17.2	0.7956	3540	1.987	18.8
(TTT conformer)	(2)	17.5	0.8160	4392	1.562	18.4
	(3)	17.7	0.8440	6029	1.081	17.4
	(4)	18.0	0.8671	6566	1.037	18.2
	(5)	16.6	0.8851	5252	0.874	12.3
	(6)	12.9	0.8789	5146	1.079	14.9
n-hexane	(1)	17.3	0.7990			
(TTT conformer)	(2)	17.6	0.8235			
	(3)	17.9	0.8532			
	(4)	18.2	0.8837			
	(5)	15.5	0.8800			
	(6)	13.6	0.8837			
cyclohexane	(1)	16.9	0.7572	1389	2.082	20.4
(C conformer)	2−3	37.1	0.8031	3346	1.523	36.0
	4−5	34.1	0.8482	3880	1.214	33.3
	(6)	11.8	0.8889	1561	0.938	10.3
cyclohexane	(1)	16.7	0.7467			
(TB conformer)	2−3	36.5	0.800			
	4−5	32.5	0.848			
	(6)	14.6	0.8822			

[a] Frozen orbital approximation. [b] Diagonal 2ph-TDA/QP level of approximation.

jugation effects.[26] Such effects favor the $C_{2s}-C_{2p}$ mixing of states for those structures exhibiting several C−H bonds oriented in a closely parallel direction. For such compounds, conformational changes are therefore essentially fingerprinted at the common border of the inner valence and outer-valence regions (i.e. in a region of the spectrum ranging from ±14 to ±22 eV).

In sufficiently extended chains, interactions of hyperconjugational character result in a net stabilization of one or several molecular orbitals at the top of the inner-valence band, by a few tenths of an electronvolt. For an ideal infinite zigzag planar chain of polyethylene, the concomitant bifurcation between states of C_{2s} and $C_{2p} + H_{1s}$ character is ruled out within the inner-valence band by the strong dispersion of the C_{2s} states and by the kinking of the carbon backbone with respect to a strictly one-dimensional structure.[27] It also leads to a significant reduction in the photoionization cross sections computed on the basis of the parametric model of Gelius for the electron levels at the top of the inner-valence band, with as a corollary a notable increase in the intensities obtained at the bottom of the outer-valence band.

These features explain the distorsion observed in the spike spectra (Figure 3) of *n*-pentane **TT** and *n*-hexane **TTT** in comparison to the symmetric distribution (Figure 7) of inner-valence energy levels produced by a simple topologocal picture. In the latter case, the dissymmetry within the calculated relative line positions (Table 1) and intensities (Table 2) can be somehow relieved (Figure 8) by twisting the chain to a **TGT** form. This conformer enables a better agreement between the theoretical and experimental inner-valence spectra, which is consistent with a partial interruption of the long-rang methylenic hyperconjugation by disordering effects in the gas phase. More precisely, from the point of view of the relative line positions and intensities at the top of the inner-valence band, the signal recorded for gaseous *n*-hexane is intermediate of those calculated for the **TTT** and **TGT** forms. This indicates that other conformations should also be taken into account. Furthermore, as contrasted with the structureless outer-valence band recorded for gaseous *n*-hexane, our simulations exhibit better-defined substructures, at different binding energies depending on the conformation. This difference also reflects a complete conformational mixing in the gas phase.

On the other hand, since the cyclic structures considered here exhibit many fewer torsional degrees of freedom than their open chain counterparts, such effects are likely to have little influence on the photoionization spectra. In the case of cyclopentane, the diagonal 2ph-TDA/QP results indicate that the distorsion to the D_{5h} planar form along the **E−HC** pseudorotation path can be detected only by a weak energy degeneracy of about 0.17 eV for the pair of energy levels at the top of the inner-valence band. Although this splitting is close to the resolution limit of the spectrum, it seems to be consistent with a slight increase, of about 0.16 eV, in the width (fwhm) of peak 4/5 in the XPS spectrum of cyclopentane with respect to the average width of peaks 4 and 5 in the XPS spectrum of *n*-pentane (Table 2). The distorsion to the planar form limits also the $C_{2s} - C_{2p} + H_{1s}$ mixing of states due to methylenic hyperconjugation effects, which explains the fact that the relative intensity attributed in the experimental spectrum to the peak $1e_{2'}$ is only reduced by a factor of 15% with respect to what should be expected considering line degeneracies only.

When considering cyclohexane, on the other hand, no torsional degree of freedom remains in the **C** conformation. Since in this case the more stable conformation is rigid, the long-range methylenic hyperconjugation can play a significant role, leading to obvious spectral features in the experimental spectrum: (i) the dissymmetric distribution of the fitted lines in the inner-valence region; (ii) a significant reduction (of about −49%) in the relative intensity attributed to the $1a_{2u}$ peak, in

(26) Castiglioni, C.; Gussoni, M.; Zerbi, G. *J. Chem. Phys.* **1991**, *95*, 7144.

(27) André, J. M. *Int. J. Quantum Chem.* **1990**, *S24*, 65.

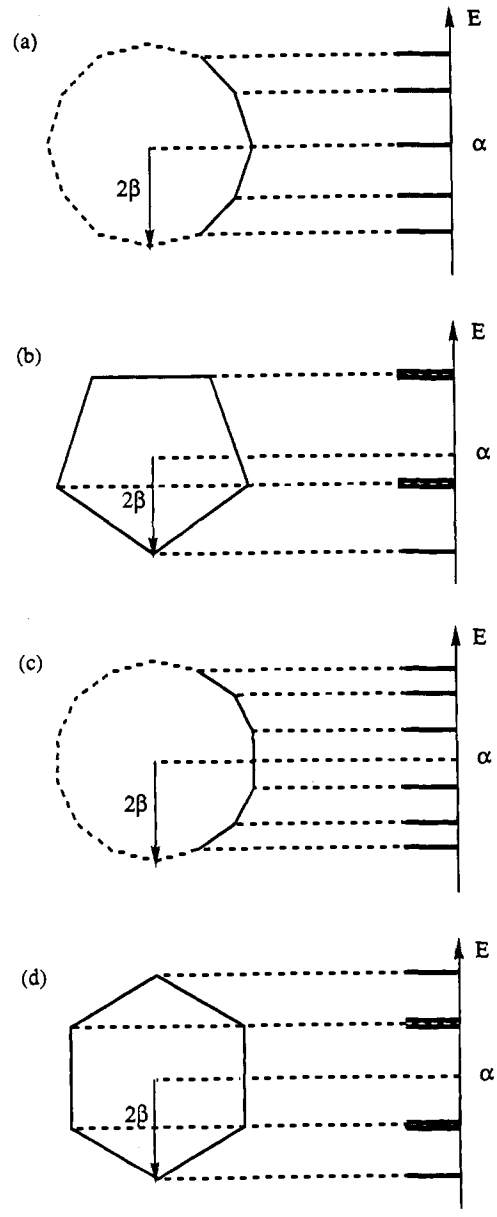

Figure 7. Hückel energy diagrams corresponding to (a) a chain of 5 vertices, (b) a cycle of 5 vertices, (c) a chain of 6 vertices, and (d) a cycle of 6 vertices.

comparison to what one might expect considering electronic degeneracies only; and (iii) in corrolary to this, a rather intense peak at about 15.1 eV, a result of a strong contamination of the $1a_{1u}$ outer-valence molecular orbital in C_{2s} atomic distributions. At this level, it is interesting to note that the ring inversion to the **TB** form, implying a complete disruption of the methylenic hyperconjugation around the cycle, should result (Figure 9) in an inner-valence band of much more symmetrical aspect and in the disappearance of the peak at 15.1 eV.

Application: Identification of Model Fold Stacking Sequences for Polyethylene Lamellae. Since direct relationships can be established between the valence electronic structure and the configuration and conformation of saturated hydrocarbons, XPS spectra can be advantageously exploited to provide information on the molecular structure at the extreme surface of related polymer samples, a region for which classical spectroscopic methods cannot be used in a definite way. Considering the structrureless signals recorded in the outer-valence region of gaseous *n*-alkane as contrasted with our simulations and with spectra obtained in the solid phase, this energy region can also be used to confirm and refine conclusions

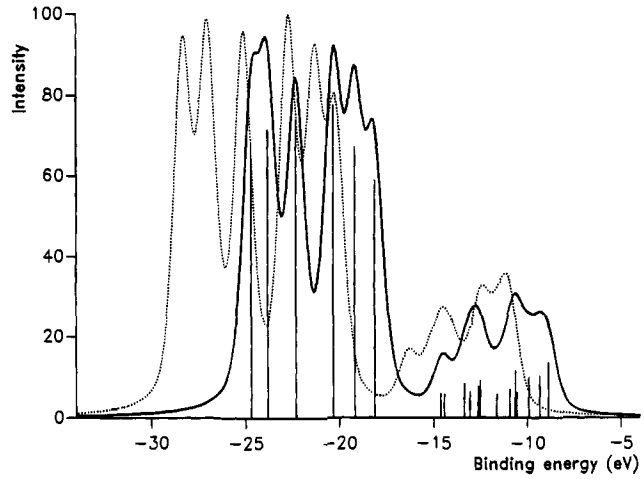

Figure 8. Simulated XPS spectrum of *n*-hexane in the **TGT** conformation at the Koopmans (···) and diagonal 2ph-TDA/QP (—) levels of approximation.

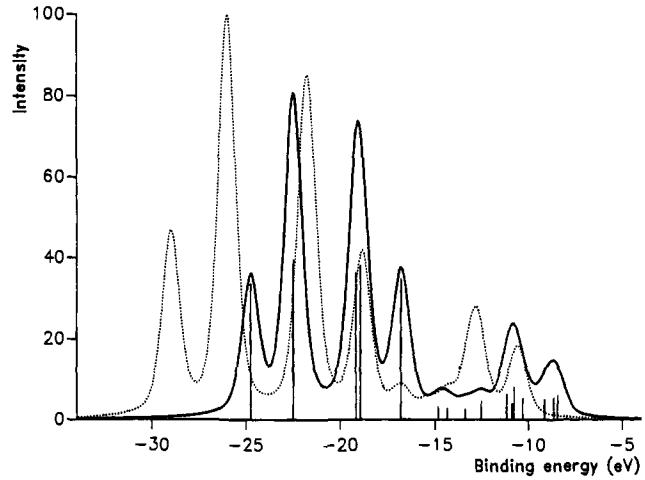

Figure 9. Simulated XPS spectrum of cyclohexane in the **TB** conformation at the Koopmans (···) and diagonal 2ph-TDA/QP (—) levels of approximation.

drawn recently from XPS inner-valence measurements on the superficial structure of polyethylene samples.

All thermodynamic theories for crystallization agree on the fact that polyethylene crystallizes in microlamellae in which the macromolecular chains emerge perpendicularly at the basal surfaces and fold back to the bulk several times. Although the existence of these folds is indirectly supported by the existence of $-CH_2-$ wagging vibrations at 1346 cm^{-1} in the infrared spectra of polyethylene lamellae,[28] or by X-ray[29] or neutron scattering[30] data on crystal grown polyethylene with controlled morphologies,[6] their nature has been and is still a controversial topic. Two extreme models, the *sharp fold*[7a] and *switchboard*[7b] models, are usually used to describe semicrystalline lamellar crystals. The sharp fold (or regular) model is characterized by a regular folding of the chains with adjacent re-entry, as depicted in Figure 1. In this model, the lamellar crystals can be considered as independent entities. In the switchboard model, on the other hand, the microlamellae are extensively intertwined

(28) Spells, S. J.; Organ, S. J.; Keller, A.; Zerbi, G. *Polymer* **1987**, *28*, 697.

(29) (a) Keller, A. *Polymer* **1962**, *3*, 393. (b) Point, J. J.; Colet, M. Ch.; Dosière, M. *J. Polym. Sci., Polym Phys.* **1986**, *24*, 345.

(30) (a) Sadler, D. M.; Keller, A. *Macromolecules* **1977**, *10*, 1128. (b) Sadler, D. M.; Keller, A. *Science* **1979**, *203*, 263. (c) Guenet, J. M. *Macromolecules* **1980**, *13*, 387. (d) Guenet, J. M. *Polymer* **1981**, *22*, 313. (e) Stamm, M.; Fischer, E. W.; Dettenmaier, M.; Convert, P. *Faraday Discuss. Chem. Soc.* **1979**, *68*, 263.

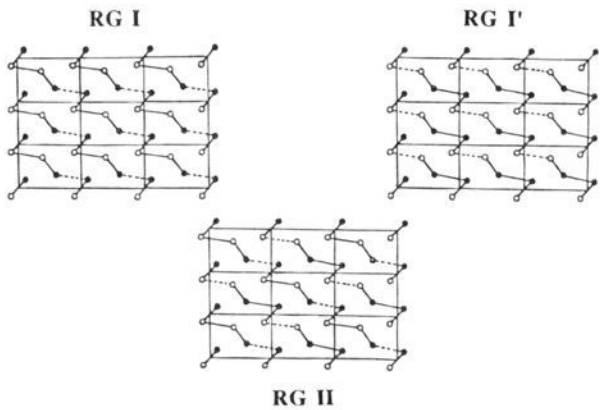

Figure 10. Ribbon stacking structure for a [110] fold surface of polyethylene. Folds are indicated by straight lines parallel to the basal planes, without any attempt to represent their actual geometry. Continuous lines (●—●) represent folds at the top surface and broken lines (○---○) folds at the bottom surface of a layer (after Basset *et al.*[32a]).

by segments of uncertain conformation in amorphous media, the adjacent re-entry of the macromolecular chains within a given lamella being much less frequent. Other intermediate models include also loose folds or dangling chain ends (cilia).

Polymer decoration experiments[31] conducted on single crystals of polyethylene have undoubtedly indicated a preferential orientation of the folds present at the basal surface, in contradiction to proposed models of the switchboard type. These surfaces must therefore essentially exhibit a regular type of fold. Furthermore, to account for some morphological features such as ridges, striations, or crackles arising from sedimentation and collapsing and for some diffraction effects given by collapsed crystals, the folds were supposed[32] earlier to pack obliquely with respect to the superficial crystalline lattice, according to one of the fold stacking sequences of Reneker and Geil[33] for the [110]'s growth sector of polyethylene (Figure 10). Thus, although the folds can reside in several conformations, these conformations all must be asymmetric. In the [110]'s growth sector, each fold connects two zigzag planar segments disposed in planes approximately perpendicular to each other, one at the corner and the other at the center of the Bunn unit cell.[34] The two most regular possible surface structures, denoted RG I (or RG I′) and RG II, consist respectively of a fully ordered repetition of asymmetrical identical (I and I′) or enantiomorphic (II) conformations. However, as polymers are grown under substantial supercooling, a random mixed stacking sequence of these two sequences is more probable. In any case, folds must take up a rather specific geometry, regardless of their chirality.

Several authors report[35] that the surface of polyethylene lamellae can be reasonably simulated with folded paraffin chains. Model structures for the folds can be inferred by analogy with the crystallographic structure of large paraffin rings.[36] In this work, the modeling of the folds is based on two conformations of a paraffin chain (Figure 11), namely Fold A and Fold B, obtained from molecular mechanics calculations.[37] The Fold A conformation is characterized by the parallel

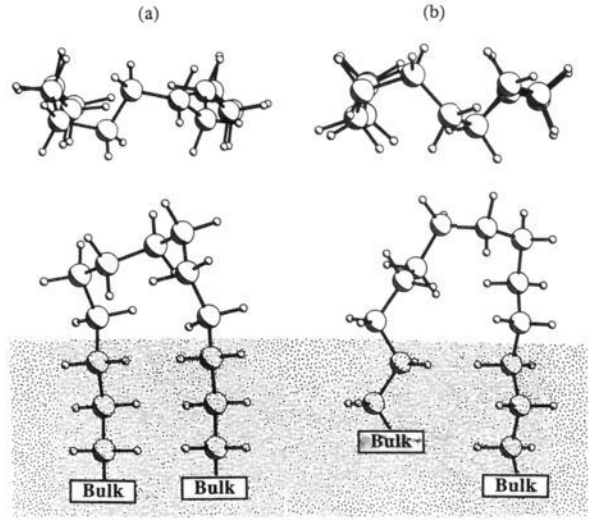

Figure 11. Selected structure for the folds, respectively (a) Fold A and (b) Fold B, represented from above (top) and an illustration (bottom) of their relationships to zigzag planar segments in the bulk.

orientation of the zigzag planar segments returning to the bulk, while within the Fold B form, these segments are twisted and fold back along planes approximately perpendicular to each other. The Fold B form is less stable than Fold A by 6.95 kJ·mol^{-1}, a weak energy difference that can be easily accommodated by the folds' environment (intermolecular forces, solvent, etc.). The vertical conformation of Fold A is representative of the superficial structure of polyethylene in the [200]'s growth sector, while the oblique conformation of Fold B has been calculated in conformity with the stacking sequences of Reneker and Geil for a [110] fold surface, similar to the one which is probed here by X-ray photoionization spectroscopy.

The XPS spectra of the Fold A and Fold B structures have been simulated (Figure 12) considering related conformers of an *n*-nonane chain. They exhibit slight but significant differences in the distribution of lines and hence in the intensities convoluted using a fwhm of 1.5 eV, reflecting an appreciable modulation of the methylenic hyperconjugation from one conformation to the other. The simulation drawn at the diagonal 2ph-TDA/QP level of aproximation for Fold B compares nicely with the experimental Al kα spectrum (Figure 13) recorded with a HP5950A spectrometer on polyethylene.[2] In spite of the somewhat arbitrary choice of the spread of the convolution function, the C_{2s} bandwidth (8.4 eV) for this structure is found to be in better agreement with the experimental value obtained (8.3 eV) than the one calculated for Fold A (8.9 eV). To point to the consistency of our approach, it is useful to recall that the C_{2s} bandwidth estimated in the same conditions[1c] for an all-staggered chain of *n*-nonane is 7.7 eV, which is also found to compare very well with the experimental value (7.6 eV) reported[38] for amorphous samples of polyethylene, exhibiting essentially long zigzag planar segments parallel to the surface.

These observations are supported by the presence of two well-separated substructures in the outer-valence band of Fold B, which fit better with the shape of the outer-valence XPS signals of the lamellae than those of Fold A. This tends to confirm Fold B as the predominating chain conformation matching the stacking sequences of Reneker and Geil for a [110] fold surface of polyethylene.

(31) Wittmann, J. C.; Lotz, B. *J. Polym. Sci.* **1985**, *23*, 205.
(32) (a) Basset, D. C.; Franck, F. C.; Keller, P. *Philos. Mag.* **1963**, *8*, 1753. (b) Basset, D. C. *Phil. Mag.* **1968**, *17*, 37.
(33) Reneker, D. H.; Geil, P. H. *J. Appl. Phys.* **1960**, *31*, 1916.
(34) Bunn, C. W. *Trans. Faraday Discuss. Soc.* **1939**, *39*, 482.
(35) See e.g.: Keller, A. *Faraday Discuss. Chem. Soc.* **1979**, *68*, 145.
(36) (a) Müller, A. *Helv. Chim. Acta* **1933**, *16*, 155. (b) Kay, H.; Newman, B. A. *Acta Crystallogr.* **1968**, *B24*, 615.
(37) Petraccone, V.; Allegra, G.; Corradini, P. *J. Polym. Sci.* **1972**, *C38*, 419.
(38) Delhalle, J.; André, J. M.; Delhalle, S.; Pireaux, J. J.; Caudano, R.; Verbist, J. J. *J. Chem. Phys.* **1974**, *60*, 585.

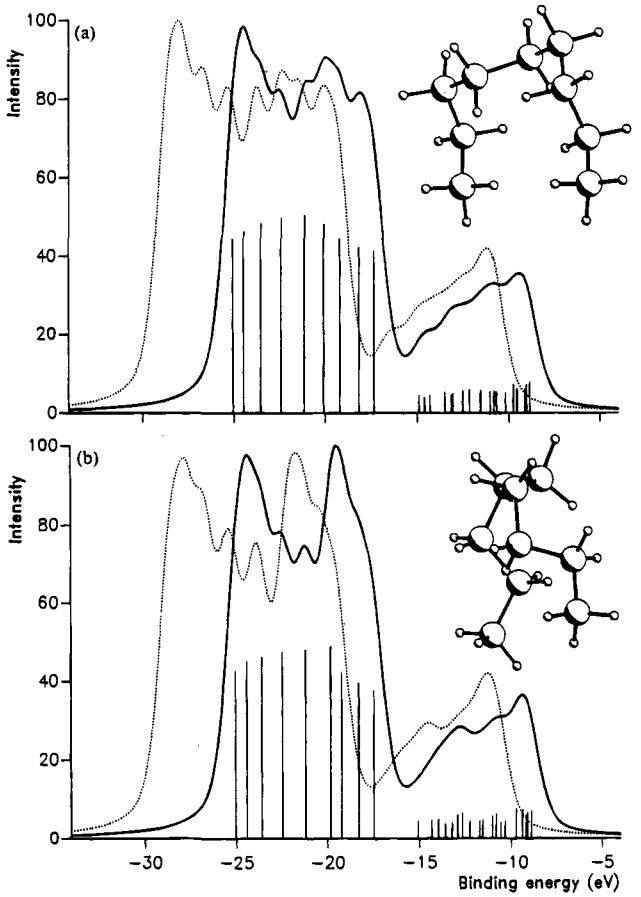

Figure 12. Theoretical XPS spectra of (a) Fold A and (b) Fold B at the Koopmans (···) diagonal 2ph-TDA/QP (—) levels of approximation.

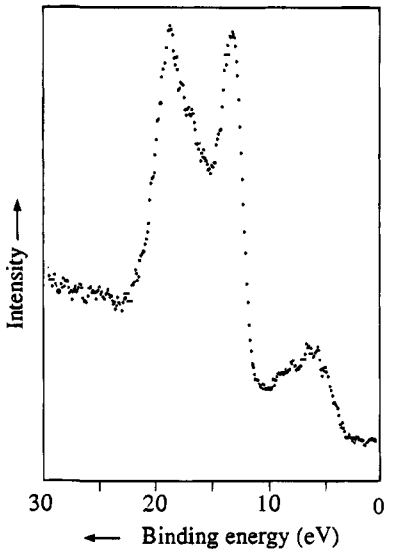

Figure 13. Valence XPS spectrum of polyethylene lamellae.

Conclusions

The goal of this work was to assess the changes induced in the electronic structure of saturated hydrocarbons by geometric effects and the extent to which they can be observed and constitute fingerprints in an XPS experiment. The XPS valence spectra of such compounds exhibit obvious configurational signatures for cyclization, resulting in numerous electronic degeneracies through the interplay of the topology of the molecular orbitals and of the torsional constraints imposed by a cyclic structure. Although the main lines at the bottom of the inner-valence band are probably subject to an appreciable fragmentation in satellite shake-up structures, the spectra recorded for *n*-pentane, *n*-hexane, cyclopentane, and cyclohexane corroborate the essential features produced by a simple tight-binding description of the inner-valence region. Diagonal 2ph-TDA calculations conducted at the quasi-particle level of approximation and using a minimal basis set also enable a satisfactory description of the primary photoionization spectra over nearly all the valence region, except for a net broadening of the peak at the top of the outer-valence band of cyclopentane. This is certainly the outcome of a strong Jahn–Teller distorsion and of the subsequent rotating vibrations in the cyclic cation.

Significant conformational signatures can also be found at the border of the inner- and outer-valence bands. These relate to the modulation of long-range methylenic hyperconjugation effects and hence of the concomitant $C_{2s} - C_{2p} + H_{1s}$ mixing of states from one conformation to the other. As contrasted with a Hückel-like symmetric distribution of states, an asymmetric dispersion of energy levels in the inner-valence band can be seen as a specific gauge of long-range methylenic hyperconjugation and can hence be exploited to identify the structures favoring those effects, such as linear zigzag planar chains or cyclic crowns. For instance, in comparison to solid phase measurements, gaseous samples of *n*-alkane compounds exhibit inner-valence bands of more symmetric aspect, which reflects severe disordering effects in the gas phase.

A corollary of the $C_{2s} - C_{2p} + H_{1s}$ mixing of states arising with hyperconjugation is the influence of the conformation on the lower part of the outer-valence band. As contrasted with solid phase measurements, the XPS outer-valence band of linear alkanes in the gas phase does not exhibit any well-defined structure, which indicates also a complex conformational mixing in the gas phase. On the other hand, for cyclohexane in the **C** form, these effects yield a peak of appreciable intensity at 15.1 eV fingerprinting this conformation, a proposition that would be worth confronting by studying different cycloalkanes connected to alkane chains in gas and solid phases.

As a direct application, the conformational influence on the outer-valence band has ultimately been used to discriminate between two models of the fold surface of polyethylene lamellae. Although they do not cope properly with solid state effects, our simulations carried out on isolated model oligomers exhibit signatures significant enough to identify the leading superficial conformation of macromolecules as a fold matching the stacking sequences of Reneker and Geil in the [110]'s growth sector of polyethylene, a 34 year old model which to our knowledge has been neither confirmed nor denied in such a direct way.

Acknowledgment. M. Deleuze is grateful to the FNRS (Belgian National Fund for Scientific Research) for his Research Assistant position. The authors thank Prof. J. M. André for his interest in this work. They acknowledge also the kind help of Dr. J. G. Fripiat (F.U.N.D.P.-Namur) and Dr. M. Grayson (University of Sheffield). All calculations reported here have been made on the Namur-Scientific Computing Facility. The authors acknowledge the support of this project within the framework of the 1993–1994 scientific agreements between the British Council (UK) and the CGRI-Communauté Française de Belgique/FNRS (Belgium). This work also has been supported in the framework of an agreement between the Belgian National Fund for Scientific Research (FRFC No. 9.4624.90 and No. 2.45119.91, FNRS-Lotto) and the Swedish Natural Science Research Council (NFR).